15th AIAA/CEAS Aeroacoustics Conference (30th AIAA Aeroacoustics Conference)
11 - 13 May 2009, Miami, Florida

AIAA 2009-3308

# Measurement of broadband noise generation on rod-airfoil-configurations

J. Giesler* and E. Sarradj #
*Aeroacoustics Group, Brandenburg University of Technology, 03046 Cottbus, Germany*

**The subject of this paper is the investigation of flow induced broadband noise generated due to unsteady loading of an airfoil. This is done in an experimental way based on acoustic measurements made on a rod-airfoil-configuration. The configuration is varied by changing the diameter of the rod and adjusting different gaps between the rod and the airfoil leading edge. Additionally, two types of airfoils are used sucessively. In total, 75 configurations are tested. All measurements are conducted in the aeroacoustic wind tunnel of the Brandenburg University of Technology at Cottbus for flow speeds between 26 m/s and 72 m/s. A 38 channel microphone array is used to record the acoustic data. The data are then processed using DAMAS, a complex beamforming algorithm. Both leading edge noise and trailing edge noise are analyzed. The results show that the noise generation on the rod-airfoil-configuration for lower frequencies depends more strongly on the varied cylinder diameters than on the width of the gap.**

## Nomenclature

| | |
|---|---|
| $Ma$ | Mach number |
| $Re$ | Reynolds number |
| $Sr$ | Strouhal number |
| $\Delta f$ | frequency line spacing [1/s] |
| $Tu$ | turbulence intensity [%] |
| $u'$ | turbulent velocity fluctuations [m/s] |
| $\overline{u}$ | mean velocity [m/s] |
| $d$ | rod diameter [m] |
| $SPL$ | sound pressure level [dB] |
| $f$ | frequency [1/s] |
| $n$ | scaling exponent |
| $c_L$ | chord length [m] |
| $S_u$ | upper Strouhal band limit |
| $S_l$ | lower Strouhal band limit |

*Subscript*

| | |
|---|---|
| $scaled$ | scaled in dependence of the flow speed |
| $Sr$ | center Strouhal number |
| $S$ | index |

## I. Introduction

Due to past progress in tonal noise reduction, broadband noise has become an important component of overall sound pressure levels radiated by many technical assemblies, e.g. fan and compressor noise of aircraft engines and noise of aircondition units. One important broadband noise generating mechanism is the interaction between the rotor wake and the leading edges of the downstream located stator blades. Additionally,

*Ph.D. student, Institute of Traffic Research, BTU Cottbus, Siemens-Halske-Ring 14, 03046 Cottbus, Germany.
#Junior Professor, Institute of Traffic Research, BTU Cottbus.

noise is generated when the turbulent vortices interact with the trailing edges of the blades.
The research project described in the paper is based on the question how the generation of broadband sound is influenced by effects of unsteady loading.
For the investigation of flow induced broadband noise an experimental setup is chosen which basically consists of a rod-airfoil-configuration. This setup is inspired by the fact that tonal as well as broadband noise is generated. Further, the configuration is suited to model important noise generating mechanisms like turbulent inflow to blades and rotor-wake-stator interactions. Another important reason is that the cylinder wake is aerodynamically well explored and described in the literature.[1,2] Because of its simplicity the configuration can easily be built and mounted in the test section of the wind tunnel.
Jacob et al.[3] used experimental acoustic results measured on a rod-airfoil setup for the verification of numerical broadband noise calculations. The same setup was also used by Nürnberger[4] to validate results of the DLR TRACE numeric code. From those publications various acoustic data exist and can be used for comparison with measurement results. Both authors describe a rod-airfoil-configuration consisting of a NACA 0012 airfoil and circular cylinders of 10 mm or 16 mm mounted 105 mm upstream of the airfoil. For both configurations the gap between rod and airfoil remained constant.
The experiments described in this paper were done in the aeroacoustic wind tunnel of the Brandenburg University of Technology at Cottbus. Airfoils of different geometry were successively placed in the wake of a circular cylinder. The diameter of the cylinder was also successively changed. Additionally, the gap between the center of the rod and the leading edge (LE) of the airfoil was varied. For different flow speeds, acoustic data were recorded with a microphone array. To analyze the noise generation, the microphone array data are processed by complex beamforming methods.
In the paper the experimental setup is described and the acoustic measurements as well as the analysis of the acoustic measurement data are explained. Further the influences of the airfoil thickness, of the rod diameter and of the gap between the center of the rod and the airfoil leading edge to the broadband noise generation are discussed. Therefore, leading edge spectra and trailing edge spectra are presented and analyzed for the varied rod-airfoil-configuration. Further the spectra are scaled in dependence of the flow speed and plotted as a function of the Strouhal number to investigate the influence of the frequency and the flow speed as a dimensionless parameter. The scaling exponent appropriate for the measured LE noise and TE noise is compared to those reported in the literature. Additionally, the LE noise and the TE noise generation is analyzed for a special Strouhal band level as a function of the dimensionless parameter x/d with x being the gap and d being the diameter of the cylinder. Based on this investigation a trend for the LE noise is found depending on the Strouhal band.

# II. Measurements

## A. Experimental Setup

A schema of the measurement setup is shown in Figure 1. It consists of a circular rod and an airfoil mounted downstream of the rod. The setup allows the variation of the flow speed, the airfoil geometry, the diameter of the cylinder and the gap between the center of the rod and the leading edge of the airfoil.

During the measurement campaign the flow speed is adjusted between 26 m/s and 72 m/s in 27 steps. This results in a Mach number range from approximately 0.08 to 0.21. Two airfoils of NACA 0012 and one of NACA 0018 type with a chord length of 100 mm and a span width of 120 mm are used. Table 1 lists the airfoils and their characteristics and Figure 2 shows a photograph of these airfoils. The Reynolds numbers based on the chord length vary between $1.64 \cdot 10^5$ and $4.56 \cdot 10^5$. One NACA 0012 airfoil and the NACA 0018 airfoil are made of aluminum whereas the second NACA 0012 airfoil is made of Accura 60, a plastic material with properties similar to polycarbonate. In the latter and in the NACA 0018 airfoil six electret microphone capsules are embedded in chord direction. The capsules are installed to measure the dynamic wall pressure fluctuations.

To achieve a variation of the airfoil inflow characteristics the diameter of the rod and the gap between the center of the rod and the airfoil LE are successively changed. Rods with 5 mm, 7 mm, 10 mm, 13 mm and 16 mm diameter all made of brass are used. The Reynolds number based on the rod diameter is between $8.2 \cdot 10^3$ and $7.3 \cdot 10^4$. The gap can be adjusted to 86 mm, 96 mm, 106 mm, 113 mm and 124 mm. A total of 75 configurations have been tested.

The setup is implemented in the aeroacoustic wind tunnel of the Brandenburg University of Technology

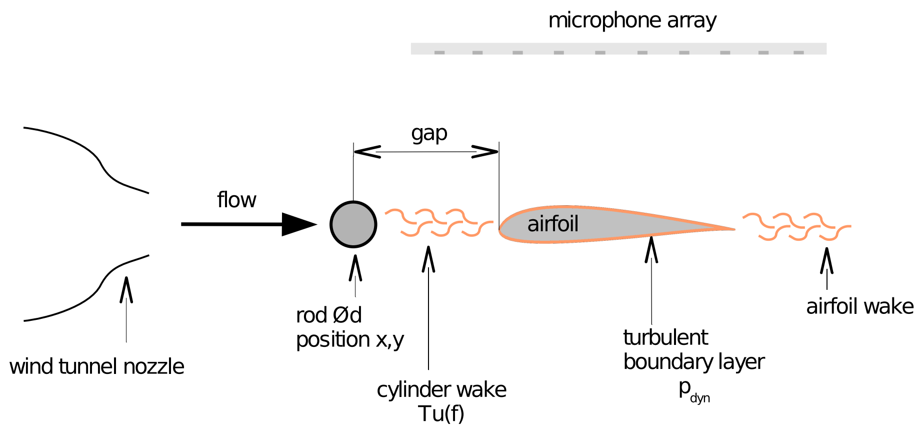


**Figure 1. Schema of the rod-airfoil-configuration.**

| Name | Type | Chord length [mm] | Span width [mm] | TE thickness [mm] | wall pressure sensors? |
|---|---|---|---|---|---|
| NACA0012-I | NACA 0012 | 100 | 120 | 0.2 | no |
| NACA0012-II | NACA 0012 | 100 | 120 | 0.7 | yes |
| NACA0018 | NACA 0018 | 100 | 120 | 0.6 | yes |

**Table 1. Overview of the airfoils successively installed in the rod-airfoil-configurations.**

at Cottbus which is an open jet wind tunnel. To achieve a low wind tunnel self noise the measuring section of this facility is located in a room separated to that including the machinery and the fan of the wind tunnel. For the experiments described in this paper a nozzle with a rectangular (120 mm x 147 mm) exit cross-section is used. With that nozzle mounted the turbulence intensity $Tu$, given by

$$Tu = \frac{\sqrt{\overline{u'^2}}}{\overline{u}} \cdot 100\% \quad , \tag{1}$$

in the core jet is below 0.2% and the A-weighted sound pressure level in 1 m distance perpendicular to the center of the nozzle is 69 dB for a flow speed of 70 m/s. A detailed description of the wind tunnel and the wind tunnel self noise and turbulence characteristics can be found in references.[5–7]
To minimize the background noise in the measurement section of the wind tunnel, the rod-airfoil-configuration

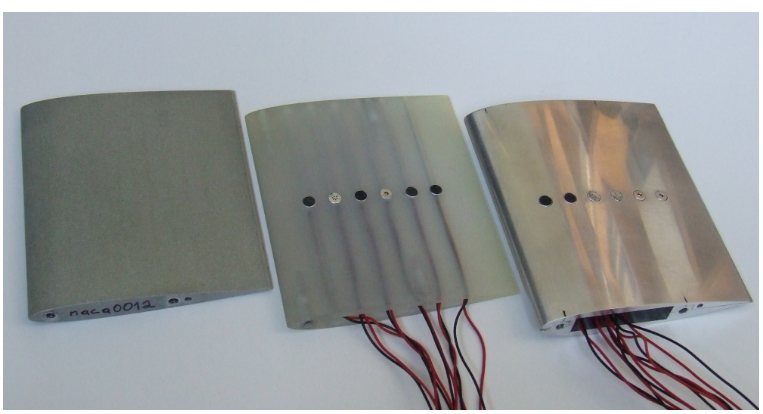

**Figure 2. Airfoils used in the experiments: Two NACA 0012 airfoils (left and middle) and one NACA 0018 airfoil (right). Two airfoils have flush integrated wall pressure sensors.**

is installed between two porous and sound absorbing side plates, directly attached to the nozzle exit. During the acoustic measurements the whole setup is surrounded by a semi anechoic enclosing of 1.6 m x 1.5 m x 2.5 m (length, with, height) size. The enclosing is lined with sound absorbing plates on three side walls and thus reduces the sound reflections for frequencies above 500 Hz. In the ceiling of the enclosing a microphone array is mounted. Figure 3 shows photographs inside the measurement room of the aeroacoustic wind tunnel (a) and of the rod-airfoil-configuration installed between two sound absorbing side plates (b).

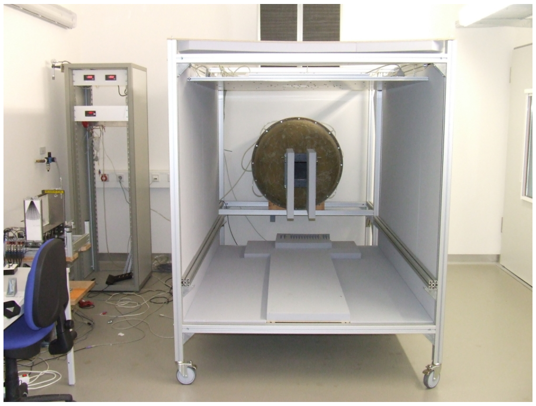

(a) Semi anechoic enclosing

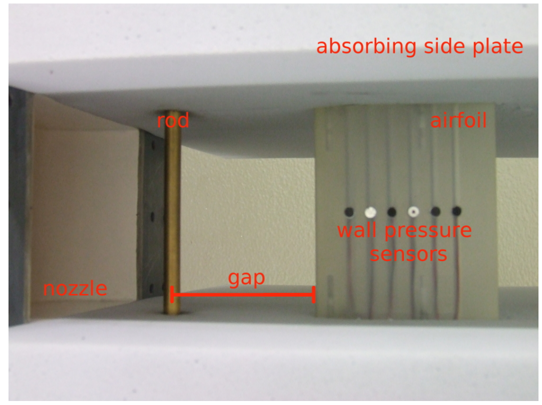


(b) Rod-airfoil-configuration between plates (top view)

**Figure 3. Measurement room of the aeroacoustic wind tunnel with semi anechoic enclosing (a) and rod-airfoil-configuration between two sound absorbing side plates directly attached to the nozzle exit (b).**

### B. Data Acquisition

The sound pressure levels of the noise generated by the different source mechanisms at different locations are the interesting parameters. To obtain as much information as possible out of the acoustic measurements a microphone array is used instead of a single microphone. Acquiring the data with a microphone array has the advantage that not only the locations and strength of the sources can be determined but also the background noise influences are minimized. Even in an aeroacoustic wind tunnel specially designed to have a low self noise and to offer a quiet measurement facility there is background noise which may influence the recording of the acoustic data. The microphone array used for the measurements described in this paper consists of 38 microphones capsules with 6 mm diameter which are flush mounted in a planar plate. It has an aperture of 1.5 m x 0.4 m. The distance between the array and the rod-airfoil plane is 72.1 cm.
The microphone array data and the wall pressure sensor data are acquired simultaneously using a 24 bit National Instruments multi channel measurement system connected to a PC. A recording time of 40 seconds and a sample rate of 51200 Hz are chosen for the capturing of the respective time historics.
For each of the 75 rod-airfoil-configurations aeroacoustic measurements were done successively for the 27 flow speeds. A total of 2300 measurements were carried out and an amount of approximately 1.7 TByte of data was recorded.

## III. Data Analysis

The microphone array data are processed by complex beamforming algorithms for frequencies between 3.4 kHz and 23 kHz in order to analyze the broadband noise emission generated at the different source locations. Below this frequency range the influence of the tonal aeolian cylinder tone cannot completely be excluded. The calculated frequency of the aeolian cylinder tone is at the maximum 2880 Hz for the configurations with the rod of 5 mm in diameter and the maximum flow speed of 72 m/s. A Hanning window and a block size of 1024 samples with an overlap of 50% are used for the Fast Fourier Transformation (FFT) in the beamforming process. The spectrum is estimated for 3999 FFT blocks and then averaged. The obtained frequency line spacing $\Delta f$ is 50 Hz. The calculations are made on a cluster of personal computers running inhouse software. The aeroacoustic results shown in this paper are based on DAMAS (deconvolution approach for the mapping of acoustic sources)[8] beamforming calculations. DAMAS is chosen after detailed testing of several other beamforming algorithms like the classical delay and sum and the orthogonal beamforming algorithm because of the obtained spatial resolution. The result of the beamforming process is a two dimensional map showing the acoustic source distribution, similar to an acoustic photograph, in the following referred to as sound map. To obtain a frequency spectrum for each noise source (rod, LE, TE) the sound map is divided into sectors corresponding to these source locations. Then, the DAMAS result is integrated over these sectors. Figure 4 exemplarily shows the three chosen sectors for the configurations with a gap of 124 mm. For the smaller gaps the sectors are arranged in the same manner but with respect to the different LE and TE positions. The sectors are arranged after analyzing the sound maps for the configurations composed of the NACA0012-I airfoil and the cylinders with diameter of 5 mm and 16 mm for all five gaps and for the maximum flow speed of 72 m/s. The definition of the TE sectors is uncritical because the noise generated at the TE can be clearly distinguished from that emitted at the rod and the LE. In comparison to that, the definition of the rod/wake sector and the LE sector is more critical. For the smaller gaps, the noise generated at the cylinder and the noise generated at the LE for some cases cannot be clearly divided in the sound maps. Thus, it is difficult to define the downstream boundary of the rod/wake sector and the upstream boundary of the LE sector. Therefore several rod/wake sectors and several LE sectors are defined which are limited by a slightly varied upstream or downstream boundary respectively. However, the comparison of the spectra calculated for the slightly varied rod and LE sectors show only very small deviations.

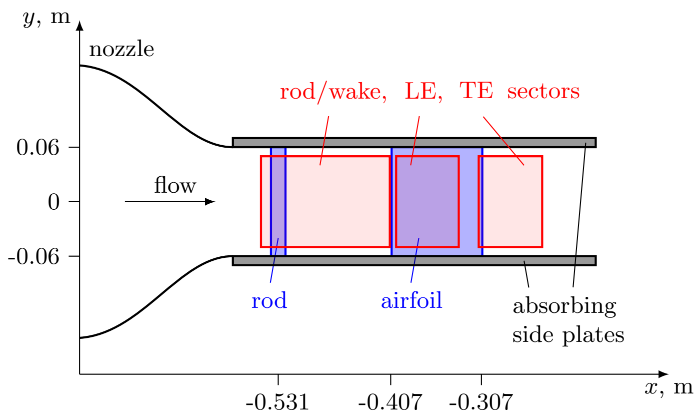


**Figure 4. Integration sectors for the rod, leading edge and trailing edge noise sources for the configurations with a gap of 124 mm.**

# IV. Results and Discussion

## A. Influence of the Airfoil Thickness

The effect of the airfoil shape on the noise generation can be seen from the results shown in Figure 5 for the 5 mm rod and the 124 mm gap. The sound pressure levels of the three noise generating mechanism rod/wake, airfoil LE and airfoil TE are compared for the NACA0018 and the two NACA 0012 airfoils. In case of the rod/wake, the sound pressure level spectra for all three airfoils show no difference except for the 4 kHz and 5 kHz third octave band, where a slight discrepancy of a few decibels exists. This indicates that the cylinder noise for frequencies above the 5 kHz third octave band is nearly not affected by exchanging the airfoil. This appears to be plausible because otherwise the influence of the airfoil on the flow has to develop downstream to interact with the rod and thus to influence the noise generated at the rod. Further it confirms that the arrangement of the rod and the LE sectors used to integrate the levels from the microphone array measurements allows the separation of both source locations.

As could be expected, the spectra for the LE noise shown in Figure 5b confirm that there is virtually no difference between the two NACA 0012. However, for the NACA0018 the LE noise found is considerably less for the frequency bands below 12.5 kHz. This is in agreement with prior experimental and theoretical results from literature (e.g. references[9,10,13]) where it is found that a bigger and blunter shape of the LE is generally responsible for a lower LE noise generation. The TE noise spectra (Figure 5c) for the two

NACA0012 are again nearly identical. The NACA0018 TE noise result is somewhat less, indicating that the turbulent boundary layer characteristics at the TE are different for this airfoil.

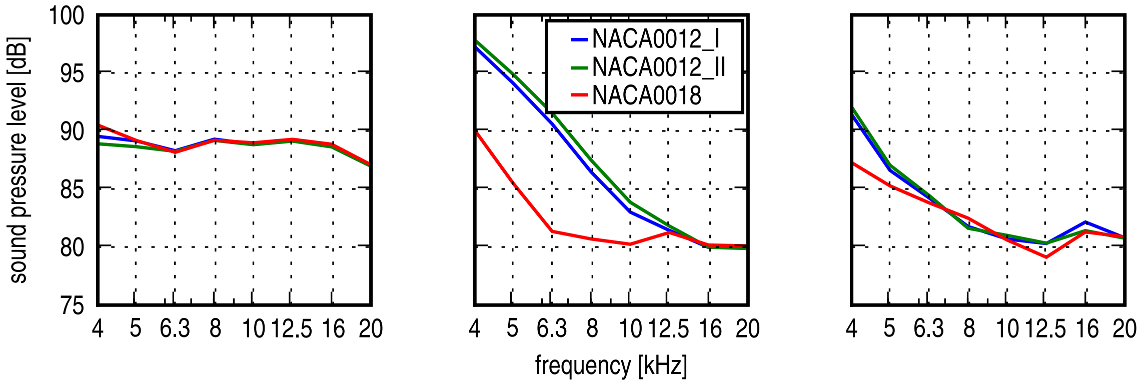


(a) Rod/wake (b) Leading edge (c) Trailing edge

**Figure 5. Third octave spectra for the three airfoils tested of the rod/wake noise (a), the leading edge noise (b) and the trailing edge noise (c). The spectra are shown for the configuration with a gap of 86 mm and a cylinder diameter of 5 mm.**

## B. Leading and Trailing Edge Noise

The noise generated at an airfoil mounted downstream of a cylinder is influenced by the diameter of the rod and by the width of the gap. To investigate these influences spectra are analyzed for the NACA0012-I configurations.

First the influence of the rod diameter will be analyzed and the sound pressure levels for the different rod diameters are compared. The spectra for the noise generated at the airfoil LE are presented in Figure 6a. It can be seen that the sound pressure levels vary mainly in the lower third octave bands (below approximately 10 kHz) and that the variation is greater for the smaller gaps. Further it can be determined for the lower third octave bands that the sound pressure levels decrease when the rod diameter increases. This could be caused by a decrease of the mean flow velocity in front of the LE. Results from hotwire measurements not shown here indicate that the mean flow velocity in front of the LE decreases when the diameter of the cylinder increases. However, the sound pressure levels for the configurations with a 7 mm rod are slightly above those for the 5 mm cylinder. Further research is necessary to fully understand this effect.

The TE spectra which are presented in Figure 6b also show variations in the lower third octave bands. But compared to the LE the variations are small. In the higher third octave bands above 10 kHz the curves of the TE sound pressure levels spread into two groups. The first group consists of the spectra of the 5 mm and 7 mm cylinder while the second group includes the spectra of the 10 mm, 13 mm and 16 mm cylinder. The level differences between these two groups are up to six decibels. Due to the lack of measurements to characterize the nature of the flow in detail this behavior cannot be explained at the moment. One possible effect that should be investigated in the future is the difference in the turbulent boundary layers probably causing different TE noise mechanisms.

Second, the influence of the gap on the noise generation shall be discussed. Again, the sound pressure levels are compared, but this time in dependence of the variation of the gap. In Figure 7a the spectra are presented for the noise generated at the airfoil LE and in Figure 7b the spectra are shown for the noise generated at the airfoil TE. The variations of the LE sound pressure levels are small compared to those of the varied rod diameter shown before. It can be seen that the TE sound pressure levels show no particular dependence on the gap width.

Comparing the spectra for the varied rod diamters (Figure 6) to those for the varied gap (Figure 7) it appears that the emitted noise on the rod-airfoil-configuration depends more on the diameter of the cylinder than on the width of the gap. The small influence of the width of the gap is in agreement with prior experimental results reported in the literature for varied rotor-stator configurations.[14,15] In those studies the dependence of the rotor-stator spacing to the noise generation was investigated. It was found that the levels of the tonal noise components were reduced in case of a greater spacing but that the levels of the broadband noise component were nearly not affected.

The according curves for the NACA0018 airfoil (not presented here) show the same qualitative behaviour. Again, the LE SPL variation is greater for the varied rod diameter than for the varied gap. In this case the variation can mainly be determined in the 4 kHz and 5 kHz third octave bands. The diagrams for the varied gap show nearly no dependence of the LE SPL to the gap.

To analyze the data in dependence of both the frequency $f$ and the flow speed $U$ the scaled SPL is plotted as a function of the dimensionless Strouhal number $Sr$, given by

$$Sr = \frac{f \cdot c_L}{U} \quad , \tag{2}$$

with $c_L$ being the chord length. The scaled sound pressure level ($SPL_{scaled}$) is normalized by $U^n$ with $U$ being the flow speed.

$$SPL_{scaled} = SPL - 10 \cdot \log_{10} \left( \frac{U}{1 \frac{\mathrm{m}}{\mathrm{s}}} \right)^n \mathrm{dB} \tag{3}$$

The diagrams are presented for the NACA0012-I and the NACA0018 configurations with a gap of 106 mm. To distinguish the different third octave band frequencies they are plotted in different colors. According to Oerlemans[9] a scaling exponent of 6.0 is chosen for the analysis of the LE noise. In Figure 8 the scaled LE SPL is presented. In case of the NACA0012-I airfoil the graphs of the scaled sound pressure levels coincide for the rod diameters of 10 mm and 13 mm. For the smaller cylinder diameters the data converge to one curve for third octave band frequencies up to 10 kHz. The spectra for the NACA0018 airfoil do not meet. Other values for the scaling exponent do not significantly improve the collapse for this case.

The according diagrams for the scaled TE SPL are shown in Figure 9. Here, a scaling exponent of $n = 5$ is used in accordance to Ffowcs-Williams and Hall[12] and Brooks, Pope and Marcolini.[11] For the NACA0012-I airfoil the scaled sound pressure levels do coincide to one curve. Only in case of the 5 mm and 7 mm cylinder the data do not converge to one graph in the two highest third octave bands.
For the NACA0018 airfoil the scaled TE sound pressure levels do not scale as well as for the NACA0012-I airfoil using the approach given in equation 3. Again, the values for the higher third octave bands do not fit. The convergence becomes better when the diameter of the cylinder increases. Other exponents do not significantly improve the collapse of the data.

To analyze the LE noise generation in dependence of the dimensionless ratio x/d a special Strouhal octave band level ($SPL_{\mathrm{Sr}}$) has been chosen. Thereby, x denotes the width of the gap and d the diameter of the rod. This Strouhal octave band level, given by

$$SPL_{Sr} = 10 \cdot \log_{10} \sum_{S=S_l}^{S_u} \left( 10^{\frac{SPL_S\left(\frac{x}{d}\right)}{10}} \right) \mathrm{dB} \quad , \tag{4}$$

is calculated as a summation of all sound pressure levels in one Strouhal octave band for each x/d ratio. The parameters $S_l$ and $S_u$ in Equation 4 denote the lower and the upper Strouhal octave band boundary. In Figure 10 the results are shown for the NACA0012-I configurations. It can be seen that the estimation of the $SPL_{Sr}$ is possible in case of the lowest octave band Strouhal number. However, for the other bands this becomes rather difficult.

## V. Conclusion

The broadband noise generation due to unsteady loading was investigated based on experiments using a variable rod-airfoil-configuration. To modify the airfoil inflow characteristics both the rod diameter and the gap between the center of the rod and the airfoil leading edge were varied successively. Additionally, three airfoils of NACA 0012 and NACA 0018 type were installed. In total 75 configurations of the rod-airfoil setup composed of cylinders with diameters ranging from 5 mm to 16 mm and gaps from 86 mm to 124 mm were tested. For each configuration the broadband noise generation were measured in the aeroacoustic wind tunnel for 27 flow speeds between 26 m/s and 72 m/s using a microphone array.

The results showed that the noise generated at the airfoil leading edge is less for the configurations with the NACA 0018 airfoil than for that with a NACA 0012 airfoil installed. Further the results indicated that the noise generated at both the leading edge and the trailing edge depends more on the cylinder diameter than on the width of the gap. This is in agreement to the results of prior analyses of rotor-stator configurations described in the literature.

For the configurations with the NACA 0012 airfoil installed the scaled sound pressure level collapsed to one curve except for the frequencies of the highest third octave band.

A special Strouhal band level was introduced to analyze the leading edge noise generation as a function of the dimensionless ratio of the gap and the diameter of the cylinder. From these analyses it can be concluded that for the lowest Strouhal octave band an approximation can be found which allows the assessment of the Strouhal octave band level. However, this becomes difficult with increasing center Strouhal numbers.

## Acknowledgments

This work is funded by the *International Graduate School of the Brandenburg University of Technology at Cottbus* (compressor technologies and materials).

## References

[1]Zdravkovich, M. M.: *Flow around Circular Cylinders; Volume 1: Fundamentals.* Oxford Science Publications, 1997.

[2]Zdravkovich, M. M.: *Flow around Circular Cylinders; Volume 2: Applications.* Oxford Science Publications, New York, 2003.

[3]Jacob, M. C.; Boudet, J.; Casalino, D.; Michard, M.: A rod-airfoil experiment as benchmark for broadband noise modeling. *Theoret. Comput. Fluid Dynamics (2005) 19: 171-196*

[4]Nürnberger, D; Ashcroft, G.: Berechnung von Breitbandlärm mit TRACE. *Deutscher Luft- und Raumfahrtkongress, 2005*

[5]Sarradj, E; Fritzsche, C.; Geyer, T. and Giesler, J.: Acoustic and aerodynamic design and characterization of a small-scale aeroacoustic wind tunnel. *Applied Acoustics, 70 (2009), pp. 1073-1080, doi:10.1016/j.apacoust.2009.02.009,* 2009.

[6]Sarradj, E.; Windisch, T.: Konzeption und Inbetriebnahme eines aeroakustischen Freistrahl-Windkanals. *Fortschritte der Akustik - DAGA 2006*

[7]Giesler, J.; Sarradj, E.: Modifikation am aeroakustischen Windkanal der BTU Cottbus. *Fortschritte der Akustik - DAGA 2008*

[8]Brooks, T. F.; Humphreys, W. M.: A deconvolution approach for the mapping of acoustic sources (DAMAS) determined from phased microphone arrays. *Journal of Sound and Vibration 294 (2006), 856879*

[9]Oerlemans, S.: Wind tunnel aeroacoustic tests of six airfoils for use on small wind turbines. *NREL report NREL/SR-500-35339, 2004*

[10]Guidati, G.: *Berechnung und Verminderung von Strömungsgeräuschen an Profilen.* PhD thesis, Universität Stuttgart, 2004.

[11]Brooks, T. F.; Pope, D. S.; Marcolini, M. A.: Airfoil Self-Noise and Prediction. *NASA Reference Publication 1218*, 1989.

[12]Ffowcs Williams, J. E.;Hall, L. H.: Aerodynamic sound generation by turbulent flow in the vicinity of a scattering halfplane. *Journal Fluid Mechanics, 40(4):657 670*, 1970.

[13]Olsen, W.; Wagner, J.: Effect of thickness on airfoil surface noise. *AIAA Journal, vol. 20, no. 3, 437-439, 1982.*

[14]Woodward, R. P.; Glaser, F. W.: Wind Tunnel Measurements of Blade/Vane Ratio snd Spacing Effects on Fan Noise. *Journal of Aircraft, vol. 20, no. 1, 58-65, 1983*

[15]Woodward, R. P; Elliott, D. M.; Hughes, C. E.; Berton, J. J.: Benefits of Swept and Leaned Stators for Fan Noise Reduction. *NASA/TM1998-208661, 1998*

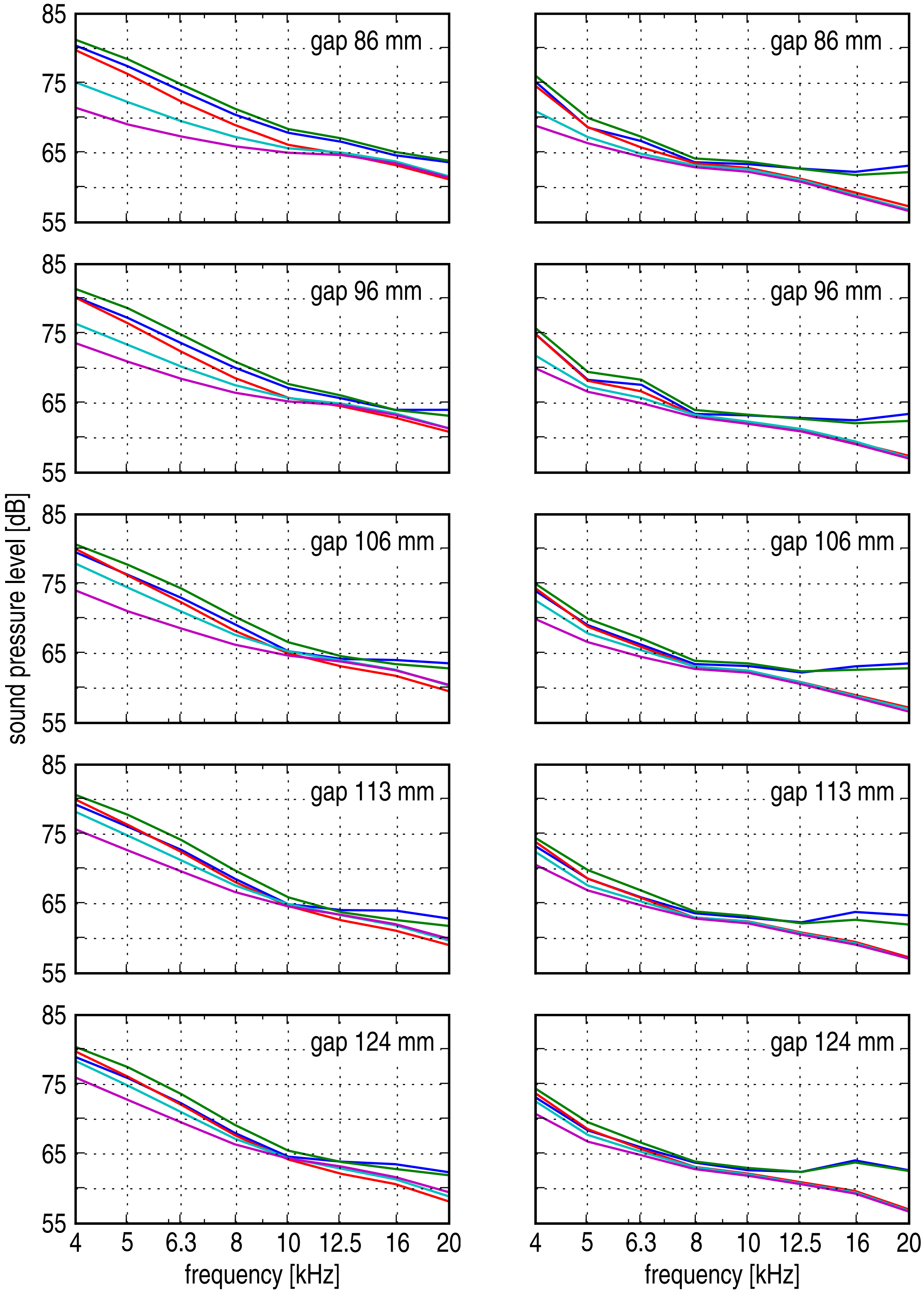


(a) Leading edge

(b) Trailing edge

**Figure 6. Third octave band spectra for the NACA0012-I airfoil shown for all gaps tested with the rod diameter as the varied parameter. The rod diameter is indicated as follows: — 5, — 7, — 10, — 13, — 16 mm.**

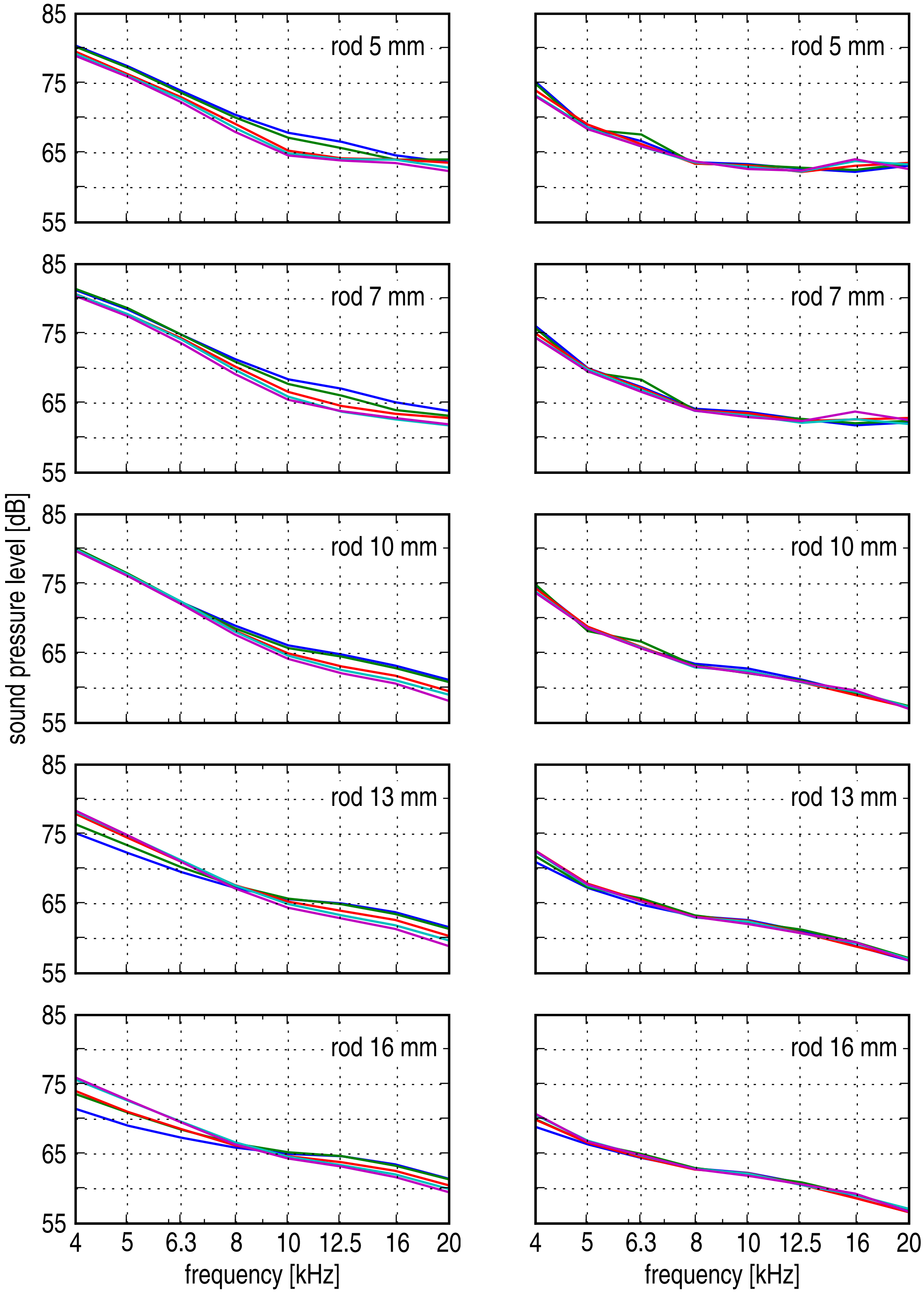


(a) Leading edge

(b) Trailing edge

**Figure 7. Third octave band spectra for the NACA0012-I airfoil shown for all tested rod diameters with the gap width as the varied parameter. The gaps are indicated as follows: — 86, — 96, — 106, — 113, — 124 mm.**

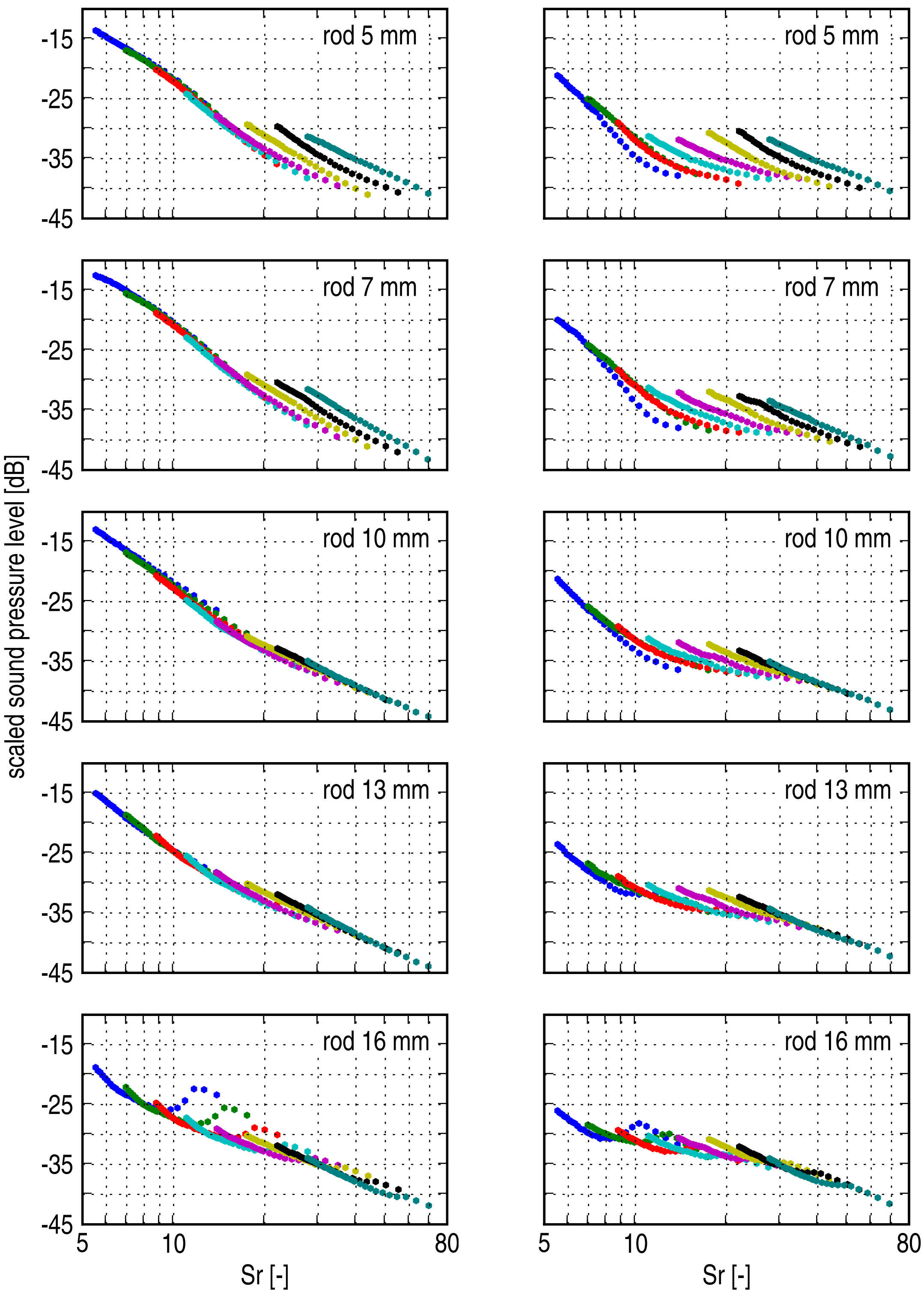


(a) NACA0012-I, levels scaled with $U^6$

(b) NACA0018, levels scaled with $U^6$

**Figure 8. Scaled sound pressure levels (Equation 3) of the leading edge noise as a function of the chord based Strouhal number. The different colors denote different third octave band frequencies: ● 4, ● 5, ● 6.3, ● 8, ● 10, ● 12.5, ● 16, ● 20 kHz.**

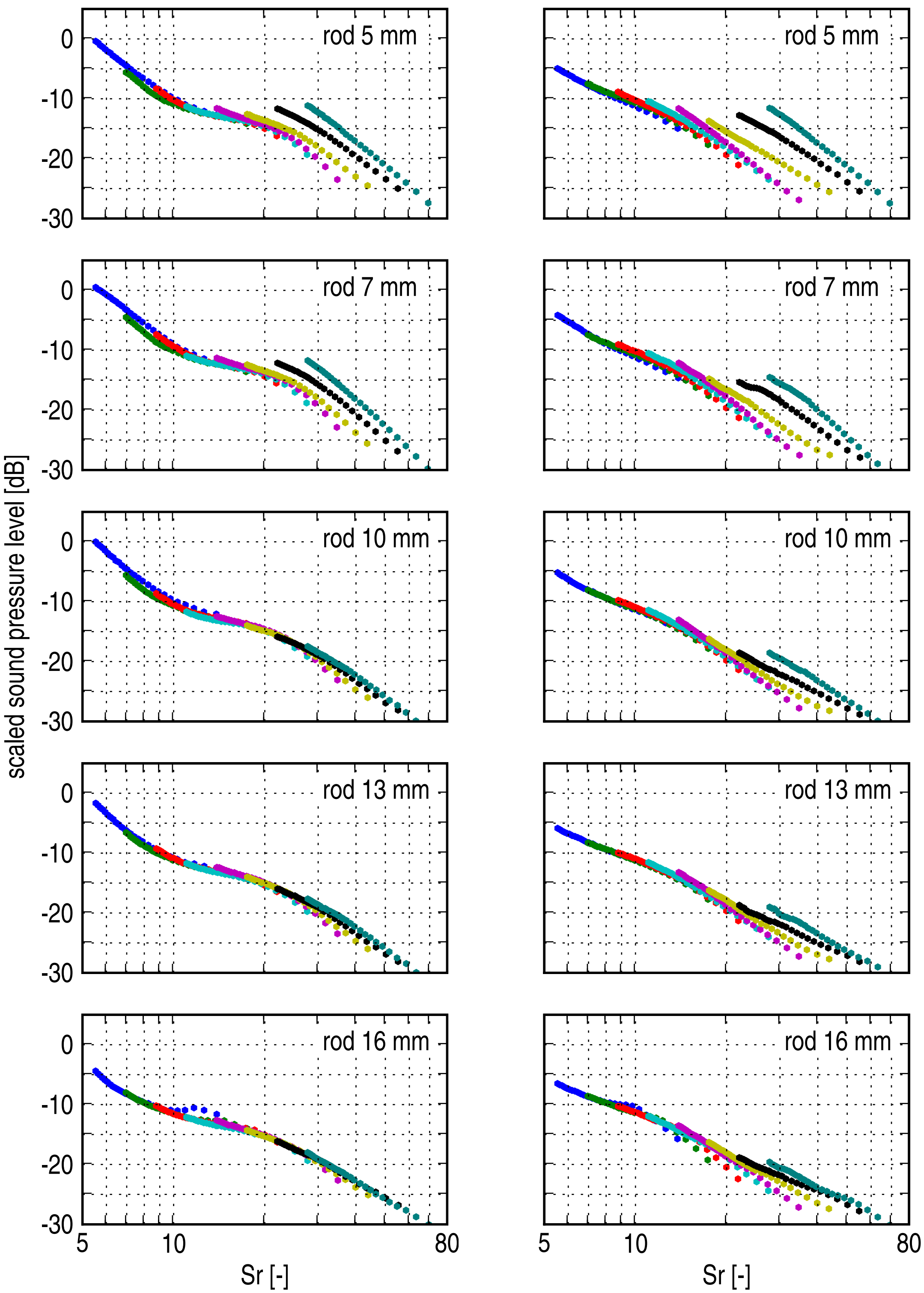


(a) NACA0012-I, levels scaled with $U^5$

(b) NACA0018, levels scaled with $U^5$

**Figure 9. Scaled sound pressure levels (Equation 3) of the trailing edge noise as a function of the chord based Strouhal number. The different colors denote different third octave band frequencies: ● 4, ● 5, ● 6.3, ● 8, ● 10, ● 12.5, ● 16, ● 20 kHz.**

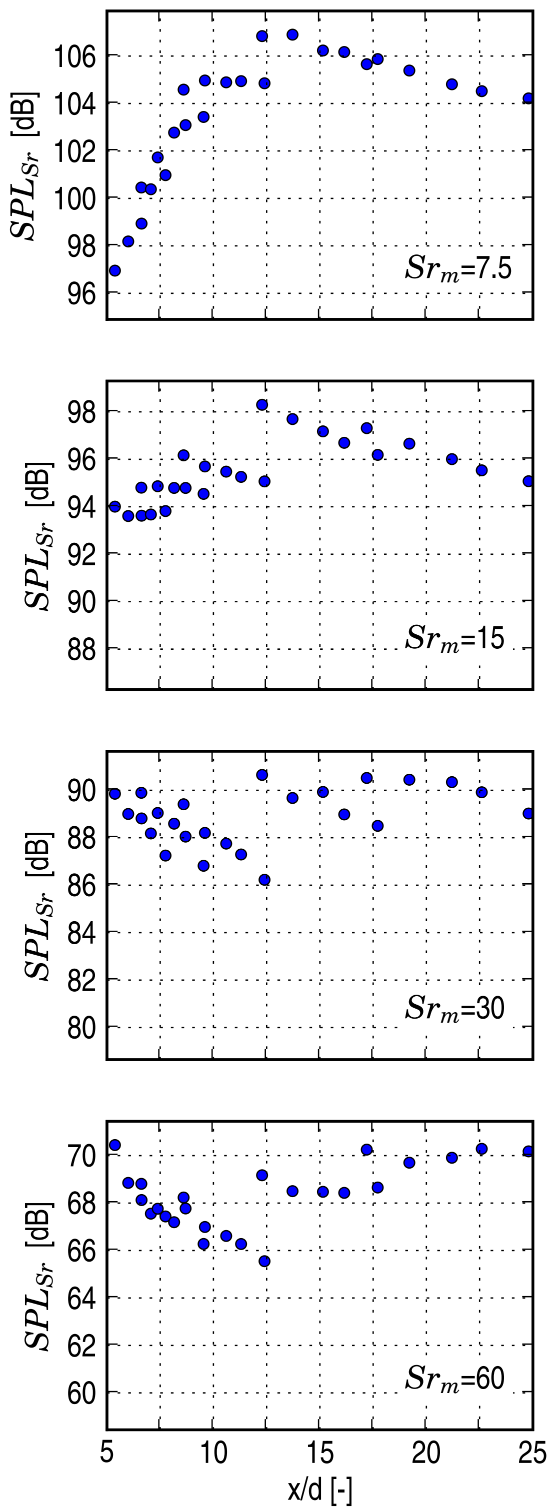


**Figure 10. Sound pressure levels for the different octave bands of the Strouhal number as a function of the dimensionless ratio x/d. The octave band center Strouhal numbers are denoted by $Sr_m$ in the diagrams.**